Review Article

Anterior segment imaging in glaucoma: An updated review

Jessica S Maslin, Yaniv Barkana[1], Syril K Dorairaj[2]

Anterior segment imaging allows for an objective method of visualizing the anterior segment angle. Two of the most commonly used devices for anterior segment imaging include the anterior segment optical coherence tomography (AS-OCT) and the ultrasound biomicroscopy (UBM). AS-OCT technology has several types, including time-domain, swept-source, and spectral-domain-based configurations. We performed a literature search on PubMed for articles containing the text "anterior segment OCT," "ultrasound biomicroscopy," and "anterior segment imaging" since 2004, with some pertinent references before 2004 included for completeness. This review compares the advantages and disadvantages of AS-OCT and UBM, and summarizes the most recent literature regarding the importance of these devices in glaucoma diagnosis and management. These devices not only aid in visualization of the angle, but also have important postsurgical applications in bleb and tube imaging.

Key words: Anterior segment imaging, anterior segment optical coherence tomography, ultrasound biomicroscopy

Access this article online

Website: www.ijo.in

DOI: 10.4103/0301-4738.169787

Quick Response Code:

Unresolved Issues and Take Home Message

- Anterior segment imaging, including AS-OCT and UBM, are objective methods of visualizing the anterior segment angle
- AS-OCT is most commonly used for appositional angle-closure and should be used when the cornea is clear and the patient can sit upright
- UBM should be used when the cornea is cloudy, for an examination in the operating room, or if plateau iris, ciliary effusion syndrome, lens subluxation, ciliary body cyst, or tumor is suspected
- Both AS-OCT and UBM are excellent for visualizing intrableb structure and glaucoma drainage device placement, and thus have important postsurgical implications
- Recent advances in anterior segment imaging include irido-trabecular contact (ITC) index, a software that can estimate the percentage of angle-closure in a given eye once the scleral spur has been manually identified
- Despite these advances in imaging, clinical examination cannot be replaced.

Visualization of the anterior chamber (AC) angle is a critical step in the diagnosis of glaucoma, especially angle-closure variants. Gonioscopy remains the clinical gold standard for the diagnosis of narrow angles; however, this method is fraught with several limitations. Gonioscopy is subjective and highly dependent on the examiner's skill and interpretation and the patient's cooperation. For example, a closed or narrow angle may erroneously appear open if too much pressure is exerted by the examiner during the dynamic gonioscopy examination or if too much light is shone into the eye.[1] Practically, many ophthalmologists do not include gonioscopy in their routine examination or even in the examination of glaucoma patients.[2,3]

Recently, the advent of anterior segment imaging devices has allowed for an objective quantitative method of analyzing the AC angle. This review will discuss the two most common types of anterior segment imaging devices, anterior segment optical coherence tomography (AS-OCT), and ultrasound biomicroscopy (UBM), and their clinical applications in the field of glaucoma.

Anterior Segment Optical Coherence Tomography

Background

The AS-OCT is a noncontact, rapid imaging device that uses low-coherence interferometry to obtain cross-sectional images of the anterior segment.[4] The measurements are semiautomated and have good reproducibility,[5,6] and, unlike gonioscopy, it is not operator dependent. The AS-OCT can be classified into time-domain (TD), swept-source (SS), and spectral-domain (SD) based configurations.[7]

Table 1 summarizes the features of each of these types. SS and SD-based imaging are considered a type of Fourier-domain (FD) OCT. Due to its inherent signal-to-noise ratio advantage, it

Department of Ophthalmology and Visual Science, Yale University School of Medicine, New Haven, Connecticut, [2]Department of Ophthalmology, Mayo Clinic, Jacksonville, Florida, USA, [1]Department of Ophthalmology, Assaf Harofeh Medical Center, Tzrifin, Israel

Correspondence to: Dr. Syril K Dorairaj, Mayo Clinic, 4500 San Pablo Road, Jacksonville, Florida 32224, USA. E-mail: dorairaj.syril@mayo.edu

Manuscript received: 26.02.15; Revision accepted: 24.05.15

Cite this article as: Maslin JS, Barkana Y, Dorairaj SK. Anterior segment imaging in glaucoma: An updated review. Indian J Ophthalmol 2015;63:630-40.

Table 1: Available types of anterior segment OCT systems

	Time-domain AS-OCT	Spectral-domain based AS-OCT	Swept-source AS-OCT
Types	Zeiss Visante Heidelberg SL-OCT	Spectralis	Casia
Central wavelength	1310 nm	830 nm	1310 nm
Axial resolution	>15 μm	<10 μm	10 μm
Imaging depth range	6-7 mm	2-3 mm	6 mm
Line-scan rate	2 kHz/200 Hz	20-40 kHz	30 kHz

AS-OCT: Anterior segment optical coherence tomography, SL-OCT: Slit-lamp optical coherence tomography

has a higher imaging speed (up to 20–40 kHz line-scan rate) than those that are based in a TD configuration. Of the TD configuration of AS-OCT, there are two common commercially available types, the Visante OCT (Carl Zeiss Meditec, Dublin, CA, USA) and the slit-lamp OCT ([SL-OCT] Heidelberg Engineering, GmbH, Dossenheim, Germany). The Visante OCT is most commonly used in the United States and has a scan speed of 2000 A-scan/s and axial resolution of 18–25 μm. It uses a 1310 nm super luminescent light-emitting diode as a light source. The scan resolution is dependent on the wavelength of the light source with shorter wavelengths allowing for higher resolution images. The downside of a shorter wavelength is that it decreases the depth penetration of the photos. The SL-OCT is only available in Europe and scans at a speed of 200 A-scan/s. Spectralis OCT (Heidelberg Engineering, Heidelberg, Germany) is an SD AS-OCT and has an axial resolution of 3.9 μm. The resolution is better on a SD-OCT. The Spectralis OCT has enhanced depth imaging (EDI), which increases the imaging sensitivity of the structures at greater depth. The SS-OCT, utilizing an SS laser wavelength of 1310 nm based on FD technology and employing a scan speed of 30,000 A-scans/s and an axial resolution of 10 μm, has recently become commercially available and is able to capture extremely high-resolution images. One that is commonly used is the Casia OCT (Tomey, Nagoya, Japan). Less than 3 s are needed to image the angle morphology in high-resolution and circumferentially 360° [Fig. 1a and b].

Compared to UBM, AS-OCT achieves better resolution and does not require contact with the ocular surface.[8] However, the use of AS-OCT is not without disadvantages. Poor agreement between gonioscopic and AS-OCT findings has been reported in the literature. Reproducibility of the AS-OCT findings in the inferior quadrant is poor, due to the variable placement of the scleral spur, especially compared with the reproducibility in the nasal and temporal angles.[9-11] The main limitation of AS-OCT is that the light energy cannot penetrate tissues behind the iris pigment epithelium, so AS-OCT cannot visualize any structures posterior to the iris pigment epithelium. Thus, AS-OCT is not useful in diagnoses such as plateau iris syndrome or phacomorphic angle-closure.

The biometric analysis of the AC angle requires a reference landmark from which the angle measurements are derived. Typically, the scleral spur is used as a reference point for parameters such as the iris area and volume,[12,13] angle opening distance (AOD),[14] angle recess area,[15] scleral thickness,[16]

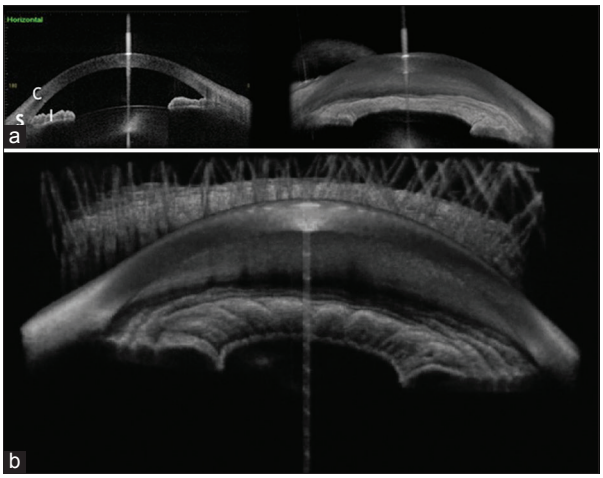

Figure 1: (a) Casia anterior segment optical coherence tomography imaging of closed angles. C: Cornea, S: Sclera, I: Iris. (b) Casia anterior segment optical coherence tomography panoramic view of peripheral anterior synechiae, 360

trabecular meshwork-ciliary process distance,[16] trabecular iris angle,[14] and trabecular iris space area.[17] Other biometric parameters that can be measured by the AS-OCT include: Iris thickness, iris curvature, AC depth, AC width, and lens vault.[18] These parameters are further described in Table 2. Difficulty in identifying the scleral spur as a reference point has been cited in numerous prior studies, with a rate of 15–28% of AS-OCT images unable to identify the scleral spur.[10,19] In the current literature, there is no consensus regarding the relationships of AS-OCT obtained measurements of the aqueous humor outflow structures to each other. One study demonstrated that the Spectralis OCT with EDI was able to identify the Schwalbe's line and scleral spur in all nasal and temporal scans.[20] In a recent study by Cheung *et al*., using a modified Cirrus SD OCT, the Schwalbe's line was identifiable in 95% of the scans and the scleral spur was identifiable in 85%.[21] In the Casia OCT, the scleral spur was identifiable in all subjects; however, Schlemm's canal was only identifiable in 32% of the scans. Its identification has also been previously reported to be subject to measurement error and variability.[8,9,16,22]

Variables such as eye quadrant,[10] a smaller AC depth, or a diagnosis of narrow angle, shorter axial length, and older age[23] can all increase the difficulty of an accurate identification of the scleral spur. As the accurate identification of the position of the scleral spur using AS-OCT is very important, several studies have investigated the techniques to best identify the scleral spur. The three most common techniques are (1) location of Schwalbe's line relative to the scleral spur, (2) the intersection of the ciliary muscle (CM) and the inner corneal margin, and (3) a bump-like structure in the inner corneal-meshwork margin. A study by Seager *et al*. demonstrated that of these three different methods, the CM approach demonstrated the highest rate of scleral spur identification with the lowest intra-observer and inter-observer variability.[24]

Anatomically narrow angles or angle-closure glaucoma

For patients with primary angle-closure glaucoma, gonioscopy has historically been the gold standard to diagnose narrow angles. AS-OCT is known to have higher sensitivity when detecting angle-closure as compared to gonioscopy.[25] An

Table 2: Biometric parameters which can be measured with the AS-OCT

Parameter	Abbreviation	Unit	Description
Iris thickness	IT	μT	Measured from a perpendicular point 500 or 750, 5m from the scleral spur, with the scleral spur defined as the point at which a change in the curvature of the inner surface of the angle is apparent
Iris cross-sectional area	IA	μA	The average of the cross-sectional area of both nasal and temporal and nasal sides
Iris curvature	IC	μC	Maximum perpendicular distance between iris pigment epithelium and line connecting the most peripheral to most central point of the epithelium
AC depth	ACD	μC	Distance from corneal endothelium to anterior surface of the lens
AC width	ACW	μC	Distance of a horizontal line joining the two scleral spurs
Angle opening distance	AOD	μO	Linear distance between the point of the inner corneoscleral wall and the iris
Angle recess area	ARA	μR	The triangular area demarcated by the anterior iris surface, corneal endothelium, and a line perpendicular to the corneal endothelium drawn from a point 750 microns anterior to the scleral spur to the iris surface
Scleral thickness	ST	μT	Measured perpendicular from the scleral spur to the episcleral surface
Trabecular meshwork-ciliary process distance	TCPD	μC	Measured from point on endothelium 500 mm from scleral spur through iris to ciliary process
Trabecular iris angle	TIA	Degrees	Angle formed from angle recess to points 500 mm from scleral spur on trabecular meshwork and perpendicular on surface of iris
Trabecular iris space area		μr	A trapezoidal area measuring the filtering area. The defining boundaries for this trapezoidal area are: anteriorly, the AOD; posteriorly, a line drawn from the scleral spur perpendicular to the plane of the inner scleral wall to the opposing iris; superiorly, the inner corneoscleral wall; and inferiorly, the iris surface
Lens vault	LV	μV	Perpendicular distance between anterior pole of the crystalline lens and the horizontal line joining the two scleral spurs

AS-OCT: Anterior segment optical coherence tomography, AC: Anterior chamber

excellent AS-OCT imaging of appositional angle-closure beginning at Schwalbe's line is shown in Fig. 2.

AS-OCT allows for better diagnosis of angle-closure glaucoma given its ease of use, nonoperator dependence, and objective measurements of important quantitative data. AS-OCT can detect clinically important changes in the AC angle structure in patients with angle-closure glaucoma under light versus dark conditions.[26]

While shallow AC depth and short axial length are known risk factors for the development of primary angle-closure glaucoma, AS-OCT has revealed that it is much more than just these two factors. Several new AS-OCT parameters have been associated with angle-closure, including smaller AC width, area, and volume;[27,28] larger lens vault;[29,30] and a greater iris thickness, curvature, and area.[31] AC area and volume and lens vault have been shown to be the most important determinants of angle width.[32] A study by Cheung *et al*. used AS-OCT to demonstrate that iris bowing is associated with angle width, independent of the AC depth.[33] AS-OCT has been used to understand the anatomic factors causing acute primary angle-closure glaucoma attacks. A recent study by Sng investigated AS-OCT measurements in 31 patients with unilateral acute primary angle-closure glaucoma prior to implementation of therapeutic interventions.[34] AS-OCT revealed that patients with acute primary angle-closure glaucoma tended to have smaller AC depth and iris curvature.[34] In pupillary block, the iris adopts a convex, forward-bowing appearance to its contour due to the pressure gradient between the AC and posterior chambers. The findings of another study in which AS-OCT was used on eyes with acute primary angle-closure glaucoma prior to therapy agreed with the above findings.[35] This study also revealed that these eyes had significantly greater lens vault compared to unaffected fellow eyes.[35]

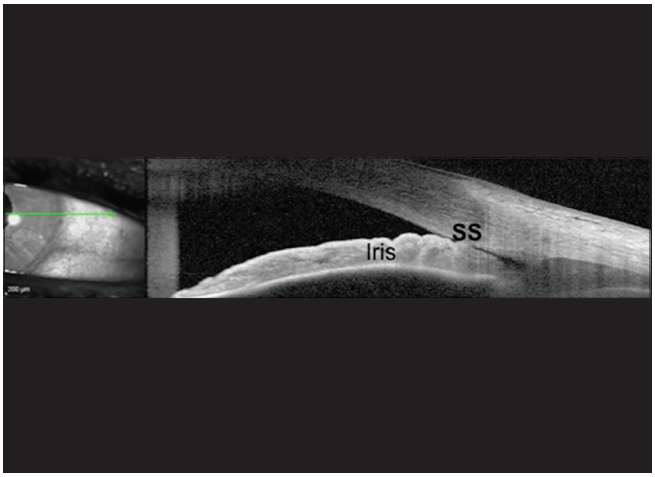

Figure 2: Anterior segment optical coherence tomography photo demonstrates S-type angle-closure with apposition beginning at Schwalbe's line. SS: Scleral spur

AS-OCT is also excellent at measuring iris parameters, which gonioscopy cannot do. Increase in iris curvature, area, and thickness has been shown to be independently associated with narrow angles in prior studies.[19,31]

AS-OCT has been used in eyes with narrow angles to demonstrate widening of the angles after laser peripheral iridotomy (LPI).[36] In addition, AS-OCT can be used to

demonstrate whether an LPI is truly patent, which is sometimes difficult to evaluate on clinical examination [Fig. 3]. A recent longitudinal study using AS-OCT to measure angle structure 2 weeks and 6 months after the procedure found that while significant angle widening was measured after LPI early after the procedure, this widening was significantly reduced to 6 months, suggesting that nonpupillary block mechanisms may contribute to primary angle-closure glaucoma.[37] A stepwise regression model with variables from these AS-OCT parameters has been shown to have a high diagnostic capability in detecting patients with angle-closure glaucoma.[38]

The SS-OCT, given its ability to provide extremely high-resolution images, has been shown to have accurate and reproducible measurements of peripheral anterior synechia (PAS), which ordinary SD-OCT cannot measure well and gonioscopy cannot measure to the same degree of precision.[39] This may allow for an excellent method of monitoring risk assessment and PAS progression in the development of angle-closure glaucoma.[39] In addition, the presence of PAS can be confirmed on SL-OCT with an indentation technique applied to the cornea.[40] SS-OCT is also excellent at calculating iris volume, which has been shown to be an important determinant of the AC angle.[41]

In the Casia, manual identification of the scleral spur can allow the user to use the irido-trabecular contact (ITC) index, software that can estimate the percentage of angle-closure in a given eye once the scleral spur has been manually identified. A recent study by Baskaran *et al.* demonstrated that the ITC index has good diagnostic performance compared to gonioscopy for estimating the degree of angle-closure.[42] Indeed, automated angle grading by software programs such as the ITC index are likely in the future for AS-OCT. AS-OCT has proven to be an important imaging device in the detection and monitoring of eyes with angle-closure glaucoma and will continue to be so in the future.

Ultrasound Biomicroscopy

Background

UBM provides high-definition, reliable, and repeatable images of the anterior segment, as well as quantitative measurements. UBM uses high frequency ultrasound at 50–100 MHz for anterior segment imaging. A computer program then converts these sound waves into a high-resolution B scan image. The probe provides a scan rate of 8 Hz, with a lateral resolution of 50 μm and an axial resolution of 25 μm.[43,44]

UBM has previously been shown to have good agreement with gonioscopy in its ability to evaluate angle-closure when performed in a darkened room.[1] In addition, there are several advantages to UBM. Unlike AS-OCT, UBM can achieve visualization of structures posterior to the iris pigment epithelium[14,43-47] as sound penetrates the pigment epithelium but light does not. Thus, UBM is better for visualizing the posterior chamber structures, including the lens zonules, ciliary body, and even the anterior choroid. Unlike AS-OCT, UBM can also be performed with the subject lying down, and thus it is useful in the operating room when an examination needs to be performed under anesthesia. Table 3 highlights the main differences between AS-OCT and UBM.

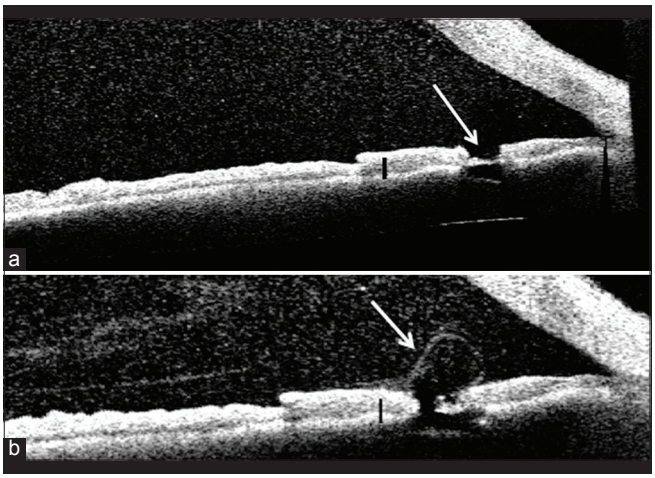

Figure 3: (a) Visante anterior segment optical coherence tomography demonstrating residual membrane occluding laser peripheral iridotomy (arrow), though iris transillumination defect is apparent on slit-lamp examination. I: Iris. (b) Following an additional neodymium: yttrium-aluminum-garnet (Nd: YAG) laser shot, the laser peripheral iridotomy is patent with a residual "burst" of pigment (arrow) demonstrated on the anterior segment optical coherence tomography. I: Iris

Table 3: Comparison of AS-OCT and UBM

AS-OCT	UBM
Noncontact	Requires contact and a liquid coupling medium
Does not require a skilled operator	Requires skilled operator
Higher axial resolution	Lower axial resolution
Limited ability to visualize structures posterior to the iris pigment epithelium	Can visualize structures posterior to the iris pigment epithelium
Faster acquisition time	Slower acquisition time
Wider field of view	Smaller field of view
Seated upright position	Seated upright or supine positions
Use for clear corneas	Can image through opaque corneas

AS-OCT: Anterior segment optical coherence tomography, UBM: Ultrasound biomicroscopy

There are some disadvantages of UBM. Prior studies have reported excellent intra-observer reproducibility but poor inter-observer reproducibility in assessing the AC angle or iris dimensions.[16,48-54] There are two recent studies that investigated the repeatability of UBM in measurement of the ciliary sulcus diameter that demonstrated that the inter-observer reproducibility had more variability than the intra-observer measurements.[55,56] In addition, UBM may have a narrower field of view compared to the AS-OCT.[17,57-59]

Manual identification of the scleral spur prior to measurements is important to the accuracy of the measurements, but there are several disadvantages to this method.[16,60] There is currently no technology available that can automatically identify the scleral spur, but some programs are semi-automatic.[61] Using the scleral spur as a reference point allows UBM to make measurements of several angle parameters, including the trabecular iris angle, the AOD,

the trabecular-ciliary process distance, iris thickness, iris ciliary process distance, iris-lens contact distance, iris zonular distance, AC angle, iris-lens angle, and AC depth.[62] Many of these parameters can also be measured with AS-OCT and are described further in Table 3.

Ultrasound biomicroscopy and glaucoma

UBM has been used to help lead further insight into the pathogenesis and mechanisms of several types of glaucoma. Indeed, because of its ability to image structures posterior to the iris, UBM has been especially useful for elucidating mechanisms of angle-closure, such as plateau iris, ciliary effusion syndrome, lens subluxation, ciliary body cyst, or tumor. Fig. 4a shows UBM of a ciliary body tumor extending up to the pars plana. On clinical examination, this patient had a pseudo-plateau iris configuration with PAS on gonioscopy [Fig. 4b].

An important study by Pavlin *et al*. demonstrated, using UBM, that those eyes with plateau iris syndrome have anteriorly situated ciliary processes.[46] UBM has been pivotal in developing further insights into this disease. It is an excellent method to clarify and confirm the clinical examination. Plateau iris has been previously defined as appearing as a relatively deep AC but with peripheral angle narrowing on gonioscopy. Notably, the angle then does not open adequately after peripheral iridotomy. In a more recent study by Mandell *et al*., they evaluated 181 eyes with plateau iris syndrome using UBM and found that the AC depth is shallower than that of normal eyes and shallower than that of eyes with pupillary block.[63] This is in contrast to previously held beliefs,[64,65] that the AC in plateau iris syndrome is deep. This previously held belief is thought to be secondary to a clinical observation of deeper AC after iridotomy, which is when plateau iris syndrome is typically diagnosed. UBM is important in plateau iris syndrome as it allows for an image of the position of the ciliary processes in relationship to the iris, and it may indeed be the most definitive method of establishing this diagnosis.[46] UBM can be used to demonstrate changes in plateau iris before and after laser iridoplasty [Fig. 5].

Pupillary block has previously been diagnosed when the iris appears bowed forward on SL biomicroscopy examination and the angle appears occludable on gonioscopy. Fig. 6 demonstrates pupillary block in lens-induced angle-closure. After peripheral iridotomy, the iris typically flattens out. This diagnosis can be confirmed with UBM as UBM allows imaging of the posterior iris epithelial surface and iris curvature.

One of the first studies to demonstrate using UBM as an adjunct to the clinical examination in the diagnosis of pupillary block syndrome was published by Aslanides in 1995 and demonstrated that UBM is a valuable tool in helping make the diagnosis of pupillary block.[66] Using UBM, a recent study by Wang *et al.* demonstrated that Chinese patients had significantly higher proportion of nonbasal iris insertion in the nasal and temporal quadrants compared to the Caucasians, and that, this difference may be a reason for their increased risk for angle-closure glaucoma.[67] Postoperatively, UBM can help distinguish pupillary block glaucoma from malignant glaucoma in cases where the exam is equivocal.[68]

For pigment dispersion syndrome, which is associated with iris concavity, UBM has been used to demonstrate that the anterior surface of the lens moves forward with accommodation.[69] It has been theorized by Pavlin *et al*. that this decrease in the AC volume increases iris concavity in patients with pigmentary dispersion syndrome.[69] A study by Potash *et al.* demonstrated through UBM imaging of 16 eyes with pigment dispersion syndrome that mid-peripheral iris concavity and iridociliary contact were associated with the disease.[70] In addition, UBM has been used to demonstrate that eyes with pigment dispersion syndrome tend to be associated with a more posterior iris insertion compared to control eyes.[71]

UBM has even been used to help characterize pseudoexfoliation syndrome. Using UBM, Guo *et al.* found that a thicker anterior lens capsule and lens zonule nodules were associated with pseudoexfoliation.[72] A paper by Sbeity *et al.* found evidence that patients with clinically unilateral pseudoexfoliation had subclinical bilateral zonular involvement as detected by UBM.[73] They suggested that UBM may be helpful to assess the zonular integrity of the fellow eye prior to cataract surgery.[73]

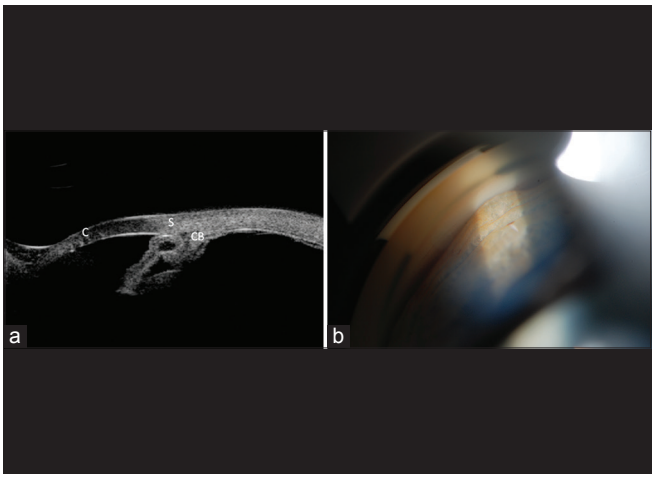

Figure 4: (a) Ultrasound biomicroscopy of a ciliary body tumor extending up to the pars plana. C: Cornea, S: Sclera, CB: Ciliary body. (b) Peripheral anterior synechiae on gonioscopy in the same patient

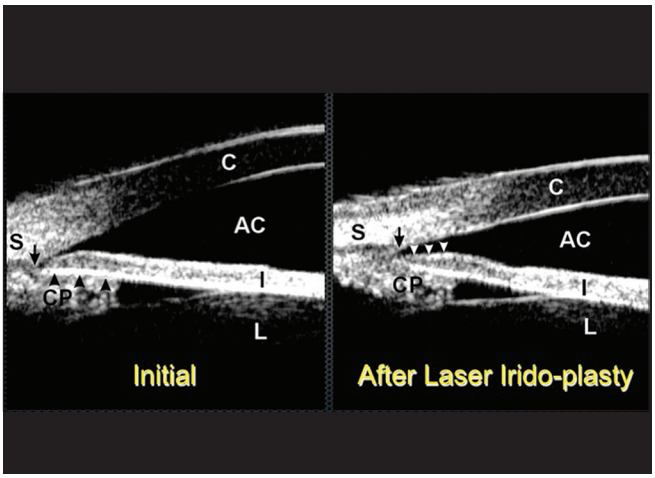

Figure 5: Ultrasound biomicroscopy of plateau iris syndrome before and after laser irido-plasty. S: Sclera, CP: Ciliary sulcus, C: Cornea, AC: Anterior chamber, I: Iris, L: Lens

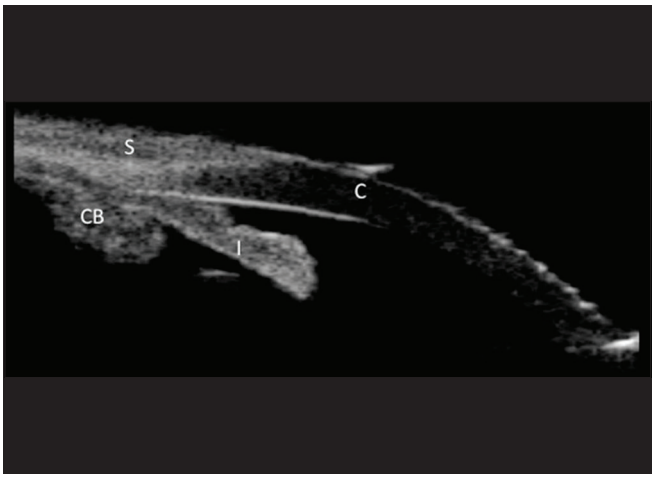

Figure 6: Ultrasound biomicroscopy in a patient with lens-induced angle-closure. CB: Ciliary body, S: Sclera, C: Cornea, I: Iris

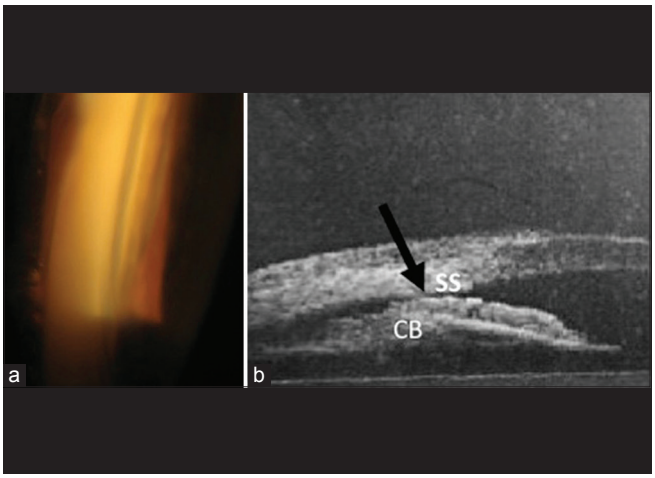

Figure 7: (a) Gonioscopy of cyclodialysis cleft. (b) Ultrasound biomicroscopy of cyclodialysis cleft demonstrating disinsertion of the ciliary body from the scleral spur (arrow). CB: Ciliary body, SS: Scleral spur

UBM has been used to provide ciliary body measurements in eyes with malignant glaucoma after trabeculectomy. A recent study by Wang *et al.* compared UBM measurements from eyes with malignant glaucoma after trabeculectomy compared to their normal fellow eyes and discovered that the ciliary bodies were thinner and more anteriorly rotated in the eyes with malignant glaucoma.[74]

Ultrasound biomicroscopy in trauma and in the evaluation of cyclodialysis clefts

UBM is helpful in evaluating eyes after ocular trauma and is especially useful when visualization is limited by media opacities or there is distortion of anterior segment anatomy.[75,76] UBM has been shown to be able to detect and localize very small ocular nonmetallic foreign bodies when computed tomography (CT) and ultrasound B scan failed to do so and can accurately determine their position relative to the sclera.[77,78] A retrospective study by Deramo *et al.* demonstrated that UBM could detect small intraocular foreign bodies <1 mm in size missed by CT and B scan.[77] In addition, UBM has been shown to be an excellent method for identifying occult zonular damage from trauma not detected on clinical examination.[79] UBM is able to detect angle recession, iridodialysis, rupture of the anterior lens capsule, lens displacement, lens subluxation, ciliary body detachment, hyphema, and traumatic cataract.[80] UBM is also able to demonstrate cyclodialysis, which is described further below.

One of the main causes of cyclodialysis, which is the disinsertion of the ciliary body from the scleral spur, is blunt trauma. Cyclodialysis may not be apparent on gonioscopy, especially in situations with hazy media, severe hypotony, or abnormal anterior segment morphology.[81,82] UBM has been helpful in diagnosing cyclodialysis cleft [Fig. 7a and b] and can even be used to confirm and observe the re-attachment of the ciliary body.[83]

Anterior Segment Imaging and Bleb Morphology

Bleb morphology has known to be an important indicator of bleb function and possible future bleb success.[84] Bleb morphology can be assessed using SL biomicroscopy for its external appearance, but SL biomicroscopy cannot assess any internal structures of the bleb. AS-OCT is useful in this regard as it can show cross-sectional images of the internal structures of the bleb. AS-OCT has been used for the imaging of trabeculectomy blebs as well as aqueous humor drainage devices. AS-OCT may be especially useful for fragile post-trabeculectomy blebs given the noncontact nature of the test.[85]

Previous studies with AS-OCT showed that mature blebs with hyporeflective walls are more likely to function.[86-88] Other additional studies demonstrated that internal fluid-filled cavities, low reflectivity of the bleb walls, microcysts, and internal ostia are associated with good filtration of the aqueous.[89,90] SD-OCT may be superior to other types of AS-OCT to visualize the superficial features of post-trabeculectomy blebs given its improved resolution.[85] In addition, AS-OCT may be useful in guiding the management and decision for laser suture lysis in post-trabeculectomy blebs.[91,92] UBM is also able to visualize these features of the bleb.[14,93,94] UBM can demonstrate the location of the scleral flap, the presence of cystic spaces, and the patency of the internal ostium [Fig. 8].[94] UBM can also demonstrate blocked internal ostium in failed bleb [Fig. 9].

A recent cross-sectional, observational study by Jung *et al.* investigated the usage of AS-OCT in the visualization of blebs from Ahmed glaucoma valves in 76 patients in order to compare the differences between successful and unsuccessful surgeries.[95] AS-OCT measurements indicated that the maximum bleb wall was significantly thinner in successful surgeries when compared to unsuccessful surgeries.[95] A recent prospective study on 56 eyes that underwent trabeculectomy analyzed the postoperative blebs at 1 month and at 6 months.[96] AS-OCT imaging that demonstrated multiform bleb wall reflectivity with a pattern of multiple internal layers and microcysts was associated with increased success of the bleb.[96] Khamar *et al.* divided bleb wall reflectivity into two types, multiform or uniform reflectivity. Multiform bleb wall reflectivity describes a bleb with small, multiple fluid-filled spaces shown as hyporeflective areas in the conjunctiva or bleb wall. It is theorized that hyporeflectivity of the bleb wall and these microcysts are collections of aqueous

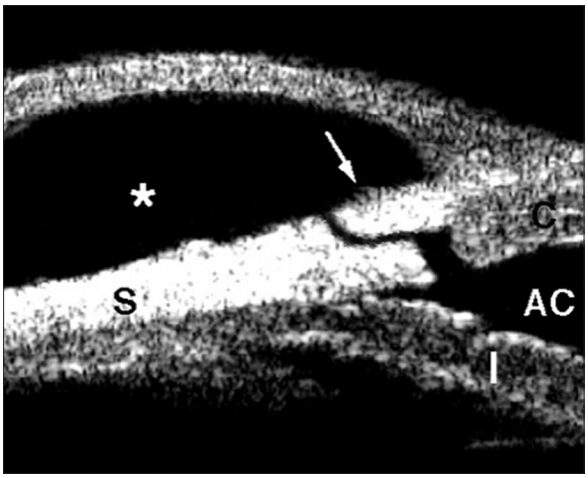

Figure 8: Ultrasound biomicroscopy of a functional filtering bleb (asterisk) with open internal ostium (arrow). S: Sclera, AC: Anterior chamber, I: Iris, C: Cornea

Figure 9: Ultrasound biomicroscopy of a failed bleb with a blocked internal ostium (arrow)

humor humor within the bleb wall. In contrast, bleb walls that have uniform reflectivity at 1 month had poor bleb function at 6 months.[96] AS-OCT may be used in the early post-operative period to predict the functionality of blebs, and thus may help indicate earlier intervention for blebs that are destined to fail.

AS-OCT is also able to produce three-dimensional (3D) images. 3D imaging has been important in classifying blebs as diffuse, encapsulated, or nonfunctioning in post-trabeculectomy eyes.[97] In addition, in these eyes, 3D AS-OCT has been shown to be important in the identification and measurement of the filtration opening on the scleral flap margin.[98] Most recently, in a prospective study by Kojima *et al*., 3D AS-OCT was used to image post-trabeculectomy blebs in 23 eyes, and various bleb parameters were measured, including position and width of filtration opening at the scleral flap, the total bleb height, fluid-filled cavity height, bleb wall thickness, and bleb wall intensity.[99] The width of the filtration opening of the bleb two t t weeks was found to be significantly correlated with intraocular pressure (IOP) at 12 months, suggesting that this parameter may be a prognostic factor for long-term IOP control.[99]

A recent case series described utilizing 3D AS-OCT guidance to perform bleb revision in two patients after trabeculectomy, one had a leaking bleb and the other had an overhanging bleb.[100] In both cases, 3D AS-OCT was essential in pinpointing the anatomical causes and guiding surgical management. Indeed, 3D AS-OCT may play a pivotal role in guiding glaucoma management in the future, in not just bleb revision, but possibly bleb needling procedures as well. In other postglaucoma surgery patients, ASOCT has been shown to be useful in diagnosing Ahmed tube tip position and patency in three patients with opaque corneas after corneal transplantation.[101] UBM may also be used to further evaluate the position of the tube [Fig. 10] and may be an important adjunct to clinical exam. With various postsurgical applications, AS-OCT has an important role in visualization of intrableb structure.

Anterior segment polarization-sensitive OCT (PS-OCT) has been used as a noninvasive method of evaluating phase retardation in blebs. PS-OCT is based on SS-OCT technology and can evaluate birefringence by imaging phase retardation of biological fibrous tissues.[102] Phase retardation is the phase difference induced by tissue birefringence. PS-OCT offers an excellent method of evaluating intrableb fibrosis not feasible with conventional AS-OCT, which may be useful in determining potential antifibrotic treatment for blebs.[102]

Conclusion

Two main imaging devices for the anterior segment, AS-OCT and UBM, offer rapid, objective, and reproducible methods to image the anterior segment. While each of these imaging devices has their advantages and disadvantages, both technologies allow the acquisition and comparison of objective data and parameters not possible with SL biomicroscopy or gonioscopy examinations. Both technologies have played important roles in furthering our understanding of the mechanisms of various types of glaucoma. While clinical examination can never be replaced by imaging devices, AS-OCT and UBM proved to be useful adjuncts to the clinical examination.

Future Directions

We anticipate that the field of anterior segment imaging will continue to grow. As more sophisticated technology is developed, anterior segment imaging will continue to have important roles in the management, diagnosis, and postsurgical management of glaucoma patients.

Salient Features

- Anterior segment imaging, including AS-OCT and UBM, are objective methods of visualizing the anterior segment angle
- AS-OCT should be used when the cornea is clear, the patient can sit upright and is most commonly used for appositional angle-closure
- AS-OCT may have higher sensitivity for detecting angle-closure than gonioscopy
- UBM should be used when the cornea is cloudy, for an examination in the operating room, or if plateau iris, ciliary effusion syndrome, lens subluxation, ciliary body cyst, or tumor is suspected

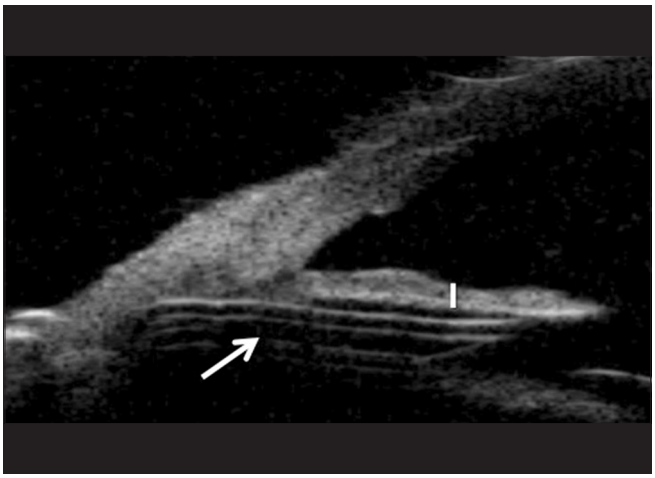

Figure 10: Ultrasound biomicroscopy of glaucoma drainage device with tube (arrow) in ciliary sulcus and blocked with iris (I)

- Both AS-OCT and UBM are excellent for visualizing intrableb structure and glaucoma drainage device placement, and thus have important postsurgical implications
- AS-OCT may be used in the early postoperative period to predict the functionality of blebs, and may indicate earlier intervention for blebs that are destined to fail
- Recent advances in anterior segment imaging include ITC index, a software that can estimate the percentage of angle-closure in a given eye once the scleral spur has been manually identified
- Anterior segment imaging can acquire objective parameters and data that are not possible with clinical examination
- Anterior segment imaging can help elucidate mechanisms of glaucoma not possible with standard clinical examination
- Despite these advances in imaging, clinical examination cannot be replaced.

Literature Search

We performed a literature search on PubMed for articles containing the text "anterior segment OCT," "ultrasound biomicroscopy," and "anterior segment imaging." Filters were used that included English only and date range from 2004 to present. These results were reviewed and only the articles deemed to be of the most clinical significance were cited in this review. Older articles cited are background information only.

Acknowledgment

The authors would like to thank Tomey Corporation for OCT images and Alison Dowdell for editorial assistance.

Financial support and sponsorship

Nil.

Conflicts of interest

There are no conflicts of interest.

References

1. Barkana Y, Dorairaj SK, Gerber Y, Liebmann JM, Ritch R. Agreement between gonioscopy and ultrasound biomicroscopy in detecting iridotrabecular apposition. Arch Ophthalmol 2007;125:1331-5.
2. Coleman AL, Yu F, Evans SJ. Use of gonioscopy in medicare beneficiaries before glaucoma surgery. J Glaucoma 2006;15:486-93.
3. Quigley HA, Friedman DS, Hahn SR. Evaluation of practice patterns for the care of open-angle glaucoma compared with claims data: The glaucoma adherence and persistency study. Ophthalmology 2007;114:1599-606.
4. Radhakrishnan S, Rollins AM, Roth JE, Yazdanfar S, Westphal V, Bardenstein DS, *et al*. Real-time optical coherence tomography of the anterior segment at 1310 nm. Arch Ophthalmol 2001;119:1179-85.
5. Shabana N, Aquino MC, See J, Ce Z, Tan AM, Nolan WP, *et al*. Quantitative evaluation of anterior chamber parameters using anterior segment optical coherence tomography in primary angle closure mechanisms. Clin Experiment Ophthalmol 2012;40:792-801.
6. Sng CC, Foo LL, Cheng CY, Allen JC Jr, He M, Krishnaswamy G, *et al*. Determinants of anterior chamber depth: The Singapore Chinese eye study. Ophthalmology 2012;119:1143-50.
7. Li P, Johnstone M, Wang RK. Full anterior segment biometry with extended imaging range spectral domain optical coherence tomography at 1340 nm. J Biomed Opt 2014;19:046013.
8. Li H, Leung CK, Cheung CY, Wong L, Pang CP, Weinreb RN, *et al*. Repeatability and reproducibility of anterior chamber angle measurement with anterior segment optical coherence tomography. Br J Ophthalmol 2007;91:1490-2.
9. Sakata LM, Lavanya R, Friedman DS, Aung HT, Gao H, Kumar RS, *et al*. Comparison of gonioscopy and anterior segment ocular coherence tomography in detecting angle closure in different quadrants of the anterior chamber angle. Ophthalmology 2008;115:769-74.
10. Sakata LM, Lavanya R, Friedman DS, Aung HT, Seah SK, Foster PJ, *et al*. Assessment of the scleral spur in anterior segment optical coherence tomography images. Arch Ophthalmol 2008;126:181-5.
11. Kim DY, Sung KR, Kang SY, Cho JW, Lee KS, Park SB, *et al*. Characteristics and reproducibility of anterior chamber angle assessment by anterior-segment optical coherence tomography. Acta Ophthalmol 2011;89:435-41.
12. Aptel F, Denis P. Optical coherence tomography quantitative analysis of iris volume changes after pharmacologic mydriasis. Ophthalmology 2010;117:3-10.
13. Quigley HA, Silver DM, Friedman DS, He M, Plyler RJ, Eberhart CG, *et al*. Iris cross-sectional area decreases with pupil dilation and its dynamic behavior is a risk factor in angle closure. J Glaucoma 2009;18:173-9.
14. Pavlin CJ, Harasiewicz K, Foster FS. Ultrasound biomicroscopy of anterior segment structures in normal and glaucomatous eyes. Am J Ophthalmol 1992;113:381-9.
15. Ishikawa H, Esaki K, Liebmann JM, Uji Y, Ritch R. Ultrasound biomicroscopy dark room provocative testing: A quantitative method for estimating anterior chamber angle width. Jpn J Ophthalmol 1999;43:526-34.
16. Tello C, Liebmann J, Potash SD, Cohen H, Ritch R. Measurement of ultrasound biomicroscopy images: Intraobserver and interobserver reliability. Invest Ophthalmol Vis Sci 1994;35:3549-52.
17. Radhakrishnan S, Goldsmith J, Huang D, Westphal V, Dueker DK, Rollins AM, *et al*. Comparison of optical coherence tomography and ultrasound biomicroscopy for detection of narrow anterior chamber angles. Arch Ophthalmol 2005;123:1053-9.
18. Sung KR, Lee KS, Hong JW. Baseline anterior segment parameters associated with the long-term outcome of laser peripheral iridotomy. Curr Eye Res 2015;40:1128-33.
19. Wang BS, Narayanaswamy A, Amerasinghe N, Zheng C, He M, Chan YH, *et al*. Increased iris thickness and association with primary angle closure glaucoma. Br J Ophthalmol 2011;95:46-50.
20. Day AC, Garway-Heath DF, Broadway DC, Jiang Y, Hayat S,

Dalzell N, *et al.* Spectral domain optical coherence tomography imaging of the aqueous outflow structures in normal participants of the EPIC-Norfolk eye study. Br J Ophthalmol 2013;97:189-95.

21. Cheung CY, Zheng C, Ho CL, Tun TA, Kumar RS, Sayyad FE, *et al.* Novel anterior-chamber angle measurements by high-definition optical coherence tomography using the Schwalbe line as the landmark. Br J Ophthalmol 2011;95:955-9.
22. Leung CK, Yung WH, Yiu CK, Lam SW, Leung DY, Tse RK, *et al.* Novel approach for anterior chamber angle analysis: Anterior chamber angle detection with edge measurement and identification algorithm (ACADEMIA). Arch Ophthalmol 2006;124:1395-401.
23. Liu S, Li H, Dorairaj S, Cheung CY, Rousso J, Liebmann J, *et al.* Assessment of scleral spur visibility with anterior segment optical coherence tomography. J Glaucoma 2010;19:132-5.
24. Seager FE, Wang J, Arora KS, Quigley HA. The effect of scleral spur identification methods on structural measurements by anterior segment optical coherence tomography. J Glaucoma 2014;23:e29-38.
25. Nolan WP, See JL, Chew PT, Friedman DS, Smith SD, Radhakrishnan S, *et al.* Detection of primary angle closure using anterior segment optical coherence tomography in Asian eyes. Ophthalmology 2007;114:33-9.
26. Masoodi H, Jafarzadehpur E, Esmaeili A, Abolbashari F, Ahmadi Hosseini SM. Evaluation of anterior chamber angle under dark and light conditions in angle closure glaucoma: An anterior segment OCT study. Cont Lens Anterior Eye 2014;37:300-4.
27. Nongpiur ME, Sakata LM, Friedman DS, He M, Chan YH, Lavanya R, *et al.* Novel association of smaller anterior chamber width with angle closure in Singaporeans. Ophthalmology 2010;117:1967-73.
28. Wu RY, Nongpiur ME, He MG, Sakata LM, Friedman DS, Chan YH, *et al.* Association of narrow angles with anterior chamber area and volume measured with anterior-segment optical coherence tomography. Arch Ophthalmol 2011;129:569-74.
29. Nongpiur ME, He M, Amerasinghe N, Friedman DS, Tay WT, Baskaran M, *et al.* Lens vault, thickness, and position in Chinese subjects with angle closure. Ophthalmology 2011;118:474-9.
30. Tan GS, He M, Zhao W, Sakata LM, Li J, Nongpiur ME, *et al.* Determinants of lens vault and association with narrow angles in patients from Singapore. Am J Ophthalmol 2012;154:39-46.
31. Wang B, Sakata LM, Friedman DS, Chan YH, He M, Lavanya R, *et al.* Quantitative iris parameters and association with narrow angles. Ophthalmology 2010;117:11-7.
32. Foo LL, Nongpiur ME, Allen JC, Perera SA, Friedman DS, He M, *et al.* Determinants of angle width in Chinese Singaporeans. Ophthalmology 2012;119:278-82.
33. Cheung CY, Liu S, Weinreb RN, Liu J, Li H, Leung DY, *et al.* Dynamic analysis of iris configuration with anterior segment optical coherence tomography. Invest Ophthalmol Vis Sci 2010;51:4040-6.
34. Sng CC, Aquino MC, Liao J, Ang M, Zheng C, Loon SC, *et al.* Pretreatment anterior segment imaging during acute primary angle closure: Insights into angle closure mechanisms in the acute phase. Ophthalmology 2014;121:119-25.
35. Lee JR, Sung KR, Han S. Comparison of anterior segment parameters between the acute primary angle closure eye and the fellow eye. Invest Ophthalmol Vis Sci 2014;55:3646-50.
36. Chalita MR, Li Y, Smith S, Patil C, Westphal V, Rollins AM, *et al.* High-speed optical coherence tomography of laser iridotomy. Am J Ophthalmol 2005;140:1133-6.
37. Jiang Y, Chang DS, Zhu H, Khawaja AP, Aung T, Huang S, *et al.* Longitudinal changes of angle configuration in primary angle-closure suspects: The zhongshan angle-closure prevention trial. Ophthalmology 2014;121:1699-705.
38. Nongpiur ME, Haaland BA, Perera SA, Friedman DS, He M, Sakata LM, *et al.* Development of a score and probability estimate for detecting angle closure based on anterior segment optical coherence tomography. Am J Ophthalmol 2014;157:32-38.e1.
39. Lai I, Mak H, Lai G, Yu M, Lam DS, Leung CK. Anterior chamber angle imaging with swept-source optical coherence tomography: Measuring peripheral anterior synechia in glaucoma. Ophthalmology 2013;120:1144-9.
40. Prata TS, Dorairaj S, De Moraes CG, Tello C, Liebmann JM, Ritch R. Indentation slitlamp-adapted optical coherence tomography technique for anterior chamber angle assessment. Arch Ophthalmol 2010;128:646-7.
41. Mak H, Xu G, Leung CK. Imaging the iris with swept-source optical coherence tomography: Relationship between iris volume and primary angle closure. Ophthalmology 2013;120:2517-24.
42. Baskaran M, Ho SW, Tun TA, How AC, Perera SA, Friedman DS, *et al.* Assessment of circumferential angle-closure by the iris-trabecular contact index with swept-source optical coherence tomography. Ophthalmology 2013;120:2226-31.
43. Pavlin CJ, Sherar MD, Foster FS. Subsurface ultrasound microscopic imaging of the intact eye. Ophthalmology 1990;97:244-50.
44. Pavlin CJ, Harasiewicz K, Sherar MD, Foster FS. Clinical use of ultrasound biomicroscopy. Ophthalmology 1991;98:287-95.
45. Wang N, Ye T, Lai M, Ou Y, Zeng M, Yang C. Comparison of results of chamber angle examination by ultrasound biomicroscopy and gonioscopy. Zhonghua Yan Ke Za Zhi 1999;35:174-8, 10.
46. Pavlin CJ, McWhae JA, McGowan HD, Foster FS. Ultrasound biomicroscopy of anterior segment tumors. Ophthalmology 1992;99:1220-8.
47. Foster FS, Pavlin CJ, Harasiewicz KA, Christopher DA, Turnbull DH. Advances in ultrasound biomicroscopy. Ultrasound Med Biol 2000;26:1-27.
48. Urbak SF, Pedersen JK, Thorsen TT. Ultrasound biomicroscopy. II. Intraobserver and interobserver reproducibility of measurements. Acta Ophthalmol Scand 1998;76:546-9.
49. Spaeth GL, Azuara-Blanco A, Araujo SV, Augsburger JJ. Intraobserver and interobserver agreement in evaluating the anterior chamber angle configuration by ultrasound biomicroscopy. J Glaucoma 1997;6:13-7.
50. Wang N, Lai M, Chen X, Zhou W. Quantitative real time measurement of iris configuration in living human eyes. Zhonghua Yan Ke Za Zhi 1998;34:369-72.
51. Yang H, Lin Z, Chen X, Wang N. Intraobserver reproducibility study of parameters for measurement of position and height of ciliary process by ultrasound biomicroscopy. Yan Ke Xue Bao 1999;15:103-6, 123.
52. Balidis MO, Bunce C, Boboridis K, Salzman J, Wormald RP, Miller MH. Intraobserver and interobserver reliability of the R/D score for evaluation of iris configuration by ultrasound biomicroscopy, in patients with pigment dispersion syndrome. Eye (Lond) 2002;16:722-6.
53. Souza Filho EC, Marigo Fde A, Oliveira C, Cronemberger S, Calixto N. Intraobserver reproducibility in anterior segment morphometry of normal eyes using ultrasound biomicroscopy (UBM). Arq Bras Oftalmol 2005;68:177-83.
54. Zhang Q, Jin W, Wang Q. Repeatability, reproducibility, and agreement of central anterior chamber depth measurements in pseudophakic and phakic eyes: Optical coherence tomography versus ultrasound biomicroscopy. J Cataract Refract Surg 2010;36:941-6.
55. Li DJ, Wang NL, Chen S, Li SN, Mu DP, Wang T. Accuracy and repeatability of direct ciliary sulcus diameter measurements by full-scale 50-megahertz ultrasound biomicroscopy. Chin Med J (Engl) 2009;122:955-9.
56. Yokoyama S, Kojima T, Horai R, Ito M, Nakamura T, Ichikawa K.

Repeatability of the ciliary sulcus-to-sulcus diameter measurement using wide-scanning-field ultrasound biomicroscopy. J Cataract Refract Surg 2011;37:1251-6.

57. Dada T, Sihota R, Gadia R, Aggarwal A, Mandal S, Gupta V. Comparison of anterior segment optical coherence tomography and ultrasound biomicroscopy for assessment of the anterior segment. J Cataract Refract Surg 2007;33:837-40.
58. Memarzadeh F, Li Y, Chopra V, Varma R, Francis BA, Huang D. Anterior segment optical coherence tomography for imaging the anterior chamber after laser peripheral iridotomy. Am J Ophthalmol 2007;143:877-9.
59. Ishikawa H, Liebmann JM, Ritch R. Quantitative assessment of the anterior segment using ultrasound biomicroscopy. Curr Opin Ophthalmol 2000;11:133-9.
60. Mou D, Fu J, Li S, Wang L, Wang X, Wu G, *et al.* Narrow- and open-angle measurements with anterior-segment optical coherence tomography and Pentacam™. Ophthalmic Surg Lasers Imaging 2010;41:622-8.
61. Lin Z, Mou da P, Liang YB, Li SZ, Zhang R, Fan SJ, *et al.* Reproducibility of anterior chamber angle measurement using the Tongren ultrasound biomicroscopy analysis system. J Glaucoma 2014;23:61-8.
62. Dada T, Gadia R, Sharma A, Ichhpujani P, Bali SJ, Bhartiya S, *et al.* Ultrasound biomicroscopy in glaucoma. Surv Ophthalmol 2011;56:433-50.
63. Mandell MA, Pavlin CJ, Weisbrod DJ, Simpson ER. Anterior chamber depth in plateau iris syndrome and pupillary block as measured by ultrasound biomicroscopy. Am J Ophthalmol 2003;136:900-3.
64. Jacobs IH. Anterior chamber depth measurement using the split-lamp microscope. Am J Ophthalmol 1979;88:236-8.
65. Wand M, Grant WM, Simmons RJ, Hutchinson BT. Plateau iris syndrome. Trans Sect Ophthalmol Am Acad Ophthalmol Otolaryngol 1977;83:122-30.
66. Aslanides IM, Libre PE, Silverman RH, Reinstein DZ, Lazzaro DR, Rondeau MJ, *et al.* High frequency ultrasound imaging in pupillary block glaucoma. Br J Ophthalmol 1995;79:972-6.
67. Wang YE, Li Y, Wang D, He M, Wu L, Lin SC. Comparison of iris insertion classification among american caucasian and ethnic Chinese using ultrasound biomicroscopy. Invest Ophthalmol Vis Sci 2013;54:3837-43.
68. Sun CB, Liu Z, Yao K. Ultrasound biomicroscopy in pupillary block glaucoma secondary to ophthalmic viscosurgical device remnants in the posterior chamber after anterior chamber phakic intraocular lens implantation. J Cataract Refract Surg 2010;36:2204-6.
69. Pavlin CJ, Macken P, Trope GE, Harasiewicz K, Foster FS. Accommodation and iridotomy in the pigment dispersion syndrome. Ophthalmic Surg Lasers 1996;27:113-20.
70. Potash SD, Tello C, Liebmann J, Ritch R. Ultrasound biomicroscopy in pigment dispersion syndrome. Ophthalmology 1994;101:332-9.
71. Kanadani FN, Dorairaj S, Langlieb AM, Shihadeh WA, Tello C, Liebmann JM, *et al.* Ultrasound biomicroscopy in asymmetric pigment dispersion syndrome and pigmentary glaucoma. Arch Ophthalmol 2006;124:1573-6.
72. Guo S, Gewirtz M, Thaker R, Reed M. Characterizing pseudoexfoliation syndrome through the use of ultrasound biomicroscopy. J Cataract Refract Surg 2006;32:614-7.
73. Sbeity Z, Dorairaj SK, Reddy S, Tello C, Liebmann JM, Ritch R. Ultrasound biomicroscopy of zonular anatomy in clinically unilateral exfoliation syndrome. Acta Ophthalmol 2008;86:565-8.
74. Wang Z, Huang J, Lin J, Liang X, Cai X, Ge J. Quantitative measurements of the ciliary body in eyes with malignant glaucoma after trabeculectomy using ultrasound biomicroscopy. Ophthalmology 2014;121:862-9.
75. Berinstein DM, Gentile RC, Sidoti PA, Stegman Z, Tello C, Liebmann JM, *et al.* Ultrasound biomicroscopy in anterior ocular trauma. Ophthalmic Surg Lasers 1997;28:201-7.
76. Genovesi-Ebert F, Rizzo S, Chiellini S, Romani A, Gabbriellini G, Sartini MS, *et al.* Ultrasound biomicroscopy in the assessment of penetrating or blunt anterior-chamber trauma. Ophthalmologica 1998;212 Suppl 1:6-7.
77. Deramo VA, Shah GK, Baumal CR, Fineman MS, Correa ZM, Benson WE, *et al.* The role of ultrasound biomicroscopy in ocular trauma. Trans Am Ophthalmol Soc 1998;96:355-65.
78. Deramo VA, Shah GK, Baumal CR, Fineman MS, Corrêa ZM, Benson WE, *et al.* Ultrasound biomicroscopy as a tool for detecting and localizing occult foreign bodies after ocular trauma. Ophthalmology 1999;106:301-5.
79. McWhae JA, Crichton AC, Rinke M. Ultrasound biomicroscopy for the assessment of zonules after ocular trauma. Ophthalmology 2003;110:1340-3.
80. Silverman RH. High-resolution ultrasound imaging of the eye – A review. Clin Experiment Ophthalmol 2009;37:54-67.
81. Endo S, Mitsukawa G, Fujisawa S, Hashimoto Y, Ishida N, Yamaguchi T. Ocular ball bullet injury: Detection of gonioscopically unrecognisable cyclodialysis by ultrasound biomicroscopy. Br J Ophthalmol 1999;83:1306.
82. Gentile RC, Pavlin CJ, Liebmann JM, Easterbrook M, Tello C, Foster FS, *et al.* Diagnosis of traumatic cyclodialysis by ultrasound biomicroscopy. Ophthalmic Surg Lasers 1996;27:97-105.
83. Kamei C, Kato T, Tsukamoto H, Mishima HK. A case of traumatic cyclodialysis followed by ultrasound biomicroscopy. Hiroshima J Med Sci 2002;51:81-4.
84. Wells AP, Crowston JG, Marks J, Kirwan JF, Smith G, Clarke JC, *et al.* A pilot study of a system for grading of drainage blebs after glaucoma surgery. J Glaucoma 2004;13:454-60.
85. Singh M, See JL, Aquino MC, Thean LS, Chew PT. High-definition imaging of trabeculectomy blebs using spectral domain optical coherence tomography adapted for the anterior segment. Clin Experiment Ophthalmol 2009;37:345-51.
86. Savini G, Zanini M, Barboni P. Filtering blebs imaging by optical coherence tomography. Clin Experiment Ophthalmol 2005;33:483-9.
87. Babighian S, Rapizzi E, Galan A. StratusOCT of filtering bleb after trabeculectomy. Acta Ophthalmol Scand 2006;84:270-1.
88. Singh M, Chew PT, Friedman DS, Nolan WP, See JL, Smith SD, *et al.* Imaging of trabeculectomy blebs using anterior segment optical coherence tomography. Ophthalmology 2007;114:47-53.
89. Leung CK, Yick DW, Kwong YY, Li FC, Leung DY, Mohamed S, *et al.* Analysis of bleb morphology after trabeculectomy with Visante anterior segment optical coherence tomography. Br J Ophthalmol 2007;91:340-4.
90. Kawana K, Kiuchi T, Yasuno Y, Oshika T. Evaluation of trabeculectomy blebs using 3-dimensional cornea and anterior segment optical coherence tomography. Ophthalmology 2009;116:848-55.
91. Singh M, Aung T, Friedman DS, Zheng C, Foster PJ, Nolan WP, *et al.* Anterior segment optical coherence tomography imaging of trabeculectomy blebs before and after laser suture lysis. Am J Ophthalmol 2007;143:873-5.
92. Singh M, Aung T, Aquino MC, Chew PT. Utility of bleb imaging with anterior segment optical coherence tomography in clinical decision-making after trabeculectomy. J Glaucoma 2009;18:492-5.
93. Yamamoto T, Sakuma T, Kitazawa Y. An ultrasound biomicroscopic study of filtering blebs after mitomycin C trabeculectomy. Ophthalmology 1995;102:1770-6.
94. McWhae JA, Crichton AC. The use of ultrasound biomicroscopy following trabeculectomy. Can J Ophthalmol 1996;31:187-91.

95. Jung KI, Lim SA, Park HY, Park CK. Visualization of blebs using anterior-segment optical coherence tomography after glaucoma drainage implant surgery. Ophthalmology 2013;120:978-83.
96. Khamar MB, Soni SR, Mehta SV, Srivastava S, Vasavada VA. Morphology of functioning trabeculectomy blebs using anterior segment optical coherence tomography. Indian J Ophthalmol 2014;62:711-4.
97. Miura M, Kawana K, Iwasaki T, Kiuchi T, Oshika T, Mori H, *et al.* Three-dimensional anterior segment optical coherence tomography of filtering blebs after trabeculectomy. J Glaucoma 2008;17:193-6.
98. Inoue T, Matsumura R, Kuroda U, Nakashima K, Kawaji T, Tanihara H. Precise identification of filtration openings on the scleral flap by three-dimensional anterior segment optical coherence tomography. Invest Ophthalmol Vis Sci 2012;53:8288-94.
99. Kojima S, Inoue T, Nakashima K, Fukushima A, Tanihara H. Filtering blebs using 3-dimensional anterior-segment optical coherence tomography: A prospective investigation. JAMA Ophthalmol 2015;133:148-56.
100. Kojima S, Inoue T, Kawaji T, Tanihara H. Filtration bleb revision guided by 3-dimensional anterior segment optical coherence tomography. J Glaucoma 2014;23:312-5.
101. Kiddee W, Trope GE. Glaucoma tube imaging using anterior segment optical coherence tomography in patients with opaque cornea. J Glaucoma 2013;22:773-5.
102. Fukuda S, Beheregaray S, Kasaragod D, Hoshi S, Kishino G, Ishii K, *et al.* Noninvasive evaluation of phase retardation in blebs after glaucoma surgery using anterior segment polarization-sensitive optical coherence tomography. Invest Ophthalmol Vis Sci 2014;55:5200-6.